

## Solvent-Dependent Molecular Structure of Ionic Species Directly Measured by Ultrafast X-Ray Solution Scattering

Kyung Hwan Kim,<sup>1,2</sup> Jae Hyuk Lee,<sup>1,2</sup> Joonghan Kim,<sup>3</sup> Shunsuke Nozawa,<sup>4</sup> Tokushi Sato,<sup>4</sup> Ayana Tomita,<sup>4</sup> Kouhei Ichiiyanagi,<sup>4</sup> Hosung Ki,<sup>1,2</sup> Jeongho Kim,<sup>5</sup> Shin-ichi Adachi,<sup>4,\*</sup> and Hyotcherl Ihee<sup>1,2,†</sup>

<sup>1</sup>Center for Nanomaterials and Chemical Reactions, Institute for Basic Science, Daejeon 305-701, Republic of Korea

<sup>2</sup>Center for Time-Resolved Diffraction, Department of Chemistry, KAIST, Daejeon 305-701, Republic of Korea

<sup>3</sup>Department of Chemistry, The Catholic University of Korea, Bucheon, 420-743, Republic of Korea

<sup>4</sup>Photon Factory, Institute of Materials Structure Science, High Energy Accelerator Research Organization (KEK), 1-1 Oho, Tsukuba, Ibaraki 305-0801, Japan

<sup>5</sup>Department of Chemistry, Inha University, Incheon, 402-751, Republic of Korea

(Received 17 January 2013; published 18 April 2013)

Ionic species often play important roles in chemical reactions occurring in water and other solvents, but it has been elusive to determine the solvent-dependent molecular structure with atomic resolution. The triiodide ion has a molecular structure that sensitively changes depending on the type of solvent and its symmetry can be broken by strong solute-solvent interaction. Here, by applying pump-probe x-ray solution scattering, we characterize the exact molecular structure of  $I_3^-$  ion in water, methanol, and acetonitrile with subangstrom accuracy. The data reveal that  $I_3^-$  ion has an asymmetric and bent structure in water. In contrast, the ion keeps its symmetry in acetonitrile, while the symmetry breaking occurs to a lesser extent in methanol than in water. The symmetry breaking of  $I_3^-$  ion is reproduced by density functional theory calculations using 34 explicit water molecules, confirming that the origin of the symmetry breaking is the hydrogen-bonding interaction between the solute and solvent molecules.

DOI: [10.1103/PhysRevLett.110.165505](https://doi.org/10.1103/PhysRevLett.110.165505)

PACS numbers: 61.05.cf, 82.30.Rs, 82.50.Hp

Ionic species play important roles in many chemical and biological reactions such as ion transfer, membrane kinetics, and acid-base equilibria [1–3]. In particular, due to the charge present in ionic species, the solute-solvent interaction sensitively changes with the type of solvent, thus affecting the structure of the ions and energy landscape of the reactions. Accordingly, aqueous solvation of ions has been a topic of intense studies [4–6]. While the effect of solvation on the ion structure and the outcome of reactions has been much studied phenomenologically, it is still challenging to describe the molecular-level change induced by solute-solvent interaction, for example, change in the structure of ionic species.

The triiodide ion ( $I_3^-$ ) in solution offers a good example that represents the role of solvent in determining the structure of ionic species [7–12]. In the gas phase and aprotic solvents, the structure is linear and symmetric with equal I–I bond lengths (Fig. 1). In contrast, in protic solvents such as water and methanol, an antisymmetric stretching mode was observed in the resonance Raman spectrum [11] and a rotationally excited  $I_2^-$  fragment was detected in the transient anisotropy measurement of photoexcited  $I_3^-$  ion [12], suggesting the existence of asymmetric (with unequal I–I bond lengths) and bent structure of the  $I_3^-$  ion, respectively. Such delicate changes of the ion structure associated with the solute-solvent interaction is called symmetry breaking, by which the naturally favorable symmetry of a system becomes lower than normal under some circumstances [13–15]. The experimental evidence for the

symmetry breaking of  $I_3^-$  ion has been supported by theoretical studies using molecular dynamics (MD) and Monte Carlo simulations [16–21].

Despite this evidence, the exact structure of the  $I_3^-$  ion has never been directly characterized experimentally. The extended x-ray absorption fine structure (EXAFS) technique was applied; it demonstrated that the peak corresponding to the I–I bond distance of  $\sim 3$  Å broadens in the protic solvents [22]. However, the symmetry breaking of  $I_3^-$  ion was not identified due to the lack of sensitivity of EXAFS at longer distances. x-ray crystallography is a powerful method for determining molecular structure in crystal [23–26], but is not applicable to a solution sample. Static x-ray solution scattering is an effective technique for determining the shape and the size of large molecules in solution, but large background scattering arising from solvent molecules obscures the details of molecular structure. For example, large-angle x-ray scattering was applied to determining the structure of small molecular systems such as binary solution and solvent-confined mesoporous materials [27–29], but its spatial resolution is not high enough for distinguishing subtle

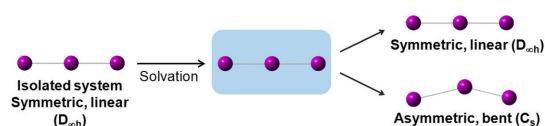


FIG. 1 (color online). Candidate structures of  $I_3^-$  ion in solution.

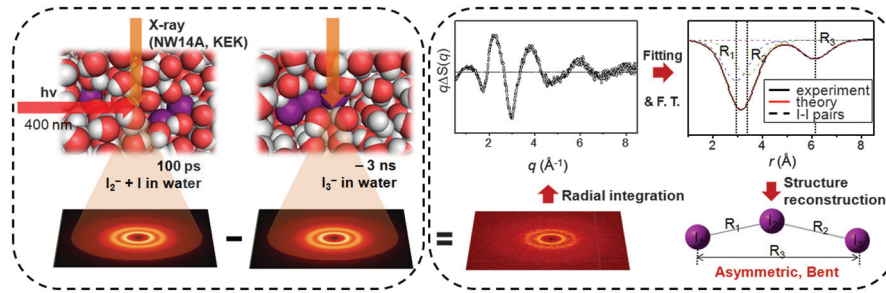


FIG. 2 (color). Schematic of our experimental method (left) and the data analysis (right). Upon irradiation at 400 nm,  $I_3^-$  ion dissociates into  $I_2^-$  and I, and the temperature of the solution increases. By taking the difference between scattering patterns measured before and 100 ps after laser excitation, only the laser-induced changes are extracted with all other background contributions being eliminated. The structural information can be extracted by the maximum likelihood estimation using five parameters (see the Supplemental Material [30] for details). Three bond distances of  $I_3^-$  can be clearly identified, giving the exact structure of  $I_3^-$  ion in various solvents.

structural changes of  $I_3^-$  ion studied in this work. In fact, we measured the static scattering of the  $I_3^-$  ion in solution, but failed to obtain a relevant scattering pattern that contains only the contribution from the solute molecules (see the Supplemental Material [30] for details).

To overcome the limited sensitivity of the static x-ray solution scattering caused by imperfect background subtraction, we applied time-resolved x-ray solution scattering (liquidography) [31–35] to the  $I_3^-$  ion in three different solvents: water ( $H_2O$ ), acetonitrile ( $CH_3CN$ ), and methanol ( $CH_3OH$ ). The key ideas of our experiment and data analysis are schematically summarized in Fig. 2. According to the previous studies [8–10] and our kinetic analysis [30], two major changes occur by 100 ps time delay when the  $I_3^-$  solution is excited by laser light at 400 nm:  $I_3^-$  ion dissociates into  $I_2^-$  and I, and the temperature of the solution increases. By taking the difference between scattering patterns measured before and 100 ps after laser excitation, only the laser-induced changes of the solution sample are extracted with all other background contributions, mainly from unreacted solute molecules, being eliminated. Since the vibrational cooling of the excited fragment ( $I_2^-$ ) is much faster than 100 ps and the recombination of  $I_2^-$  and I is much slower than 100 ps, the changes related with those processes are irrelevant in our experimental data. To extract the structure of the  $I_3^-$  ion from the difference scattering intensity, the maximum likelihood estimation with a chi-square estimator was employed [36–38] with five variable parameters (see the Supplemental Material [30]). The parameters are three bond distances for the  $I_3^-$  ion ( $R_1$ ,  $R_2$ , and  $R_3$  for the distance between  $I_1$  and  $I_2$ ,  $I_2$  and  $I_3$ ,  $I_1$  and  $I_3$ , respectively, as shown in Fig. 2), the bond distance for the  $I_2^-$  fragment ( $R_4$ ), and temperature change. The theoretical scattering patterns were calculated by considering solute contribution, solvent hydrodynamics, and the contribution from solute-solvent interaction (cage). These three contributions were obtained by the Debye equation, a separate solvent-heating experiment, and the pair-distribution functions

calculated from MD simulation, respectively. As a result, the lengths of the three bonds in the  $I_3^-$  ion are identified with subangstrom accuracy, allowing us to determine the exact structure of the  $I_3^-$  ion in solution. The details of the experimental procedure and analysis are described in the Supplemental Material [30] and our previous publications [39–42].

To reveal the symmetry breaking of the  $I_3^-$  ion induced by hydrogen-bonding interaction with the solvent, the structure of the  $I_3^-$  ion was characterized in three different solvents. The solvents of water, acetonitrile, and methanol have two, zero, and one functional groups available for hydrogen bonding, respectively. Figure 3 shows

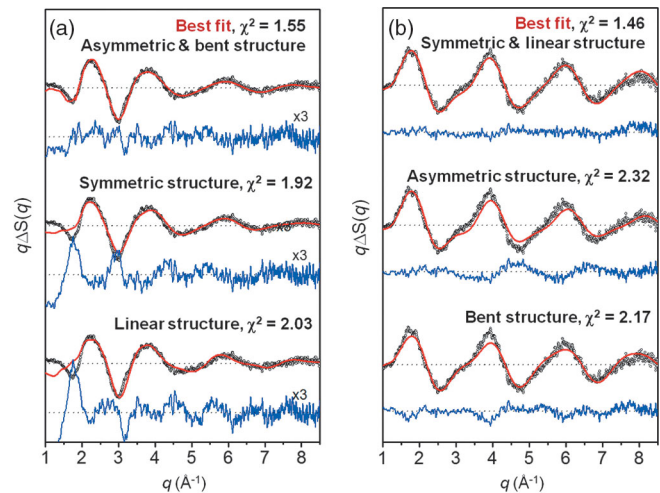


FIG. 3 (color). Difference scattering curves from the  $I_3^-$  photolysis in water and acetonitrile solutions. Experimental (black) and theoretical (red) curves using various candidate structures of  $I_3^-$  ion are compared. Residuals (blue) obtained by subtracting the theoretical curve from the experimental one are displayed at the bottom. (a) In water,  $I_3^-$  ion was found to have an asymmetric and bent structure. To emphasize the fine difference in fitting quality, the residuals shown were multiplied by a factor of 3. (b) In acetonitrile,  $I_3^-$  ion was found to have a symmetric and linear structure.

experimental and theoretical difference scattering curves at 100 ps for the  $I_3^-$  ion in water and acetonitrile solutions. In the water solution, the asymmetric ( $R_1 > R_2$ ) and bent ( $R_1 + R_2 > R_3$ ) structure of the  $I_3^-$  ion gave the best fit when every parameter was adjusted freely. If a symmetric structure ( $R_1 = R_2$ ) or a linear structure ( $R_1 + R_2 = R_3$ ) is assumed as a constraint, the fit between theory and experiment deteriorates. In contrast, in acetonitrile, the symmetric ( $R_1 = R_2$ ) and linear ( $R_1 + R_2 = R_3$ ) structure gave the best fit within the error range when every parameter was adjusted freely. If an asymmetric structure ( $R_1 > R_2$ ,  $R_1 = 1.1R_2$ ) or a bent structure ( $R_1 + R_2 > R_3$ ,  $R_1 + R_2 = 1.05R_3$ ) is assumed as a constraint, the agreement deteriorates. The optimized structure in methanol lies in between the ones in water and acetonitrile solutions, as expected from the number of functional groups available for hydrogen bonding. The optimized structure was slightly asymmetric and the quality of the fit also became worse when the symmetric constraint was used. However, in contrast to the bent structure predicted by femtosecond spectroscopy, the linear structure ( $R_1 + R_2 = R_3$ ) was obtained from our analysis. This discrepancy can be attributed to the smaller bending angle of the ion structure in methanol than in water and the relatively large error of the x-ray solution scattering at distances larger than 6 Å (see the Supplemental Material [30]). Optimized bond distances and their errors are summarized in Table I.

The distinction between the different structures of the  $I_3^-$  ion can be emphasized when the contribution of  $I_3^-$  alone is extracted by subtracting the contributions of  $I_2^-$  ion, temperature change of solvent, and the cage component. Figure 4 shows the extracted real-space features of only the  $I_3^-$  ion in water and acetonitrile solutions. Each experimental curve (black line) can be fit by a sum of contributions from three I-I distances (red line) optimized in the fitting analysis described in Fig. 3. Interestingly, for the peak around 3 Å, the peak is broader in water than in acetonitrile. This observation indicates that  $I_3^-$  ion in water has two different I-I bond distances around 3 Å and thus have an asymmetric structure. The asymmetric structure of  $I_3^-$  in water is supported by the poor fit when using a symmetric structure [middle panel of Fig. 4(a)]. The peak centered at  $\sim 6$  Å, which corresponds to the distance between the two end atoms,  $R_3$ , can be used for

determining whether  $I_3^-$  ion has a linear or bent structure. In water,  $R_3$  (6.13 Å) is shorter than the sum of  $R_1$  and  $R_2$  (6.31 Å), indicating the bent structure of  $I_3^-$ . If a linear structure is forced by using  $R_3 = 6.31$  Å, the peak positions of the experimental and theoretical curves do not match well [bottom panel of Fig. 4(a)].

The results from the acetonitrile solution can be explained in the same manner. If an asymmetric structure of the  $I_3^-$  ion with two different bond lengths (2.84 and 3.15 Å) is used, the theoretical curve has a broader width than the experimental data [middle panel of Fig. 3(b)]. The distance between the end atoms (5.99 Å) is the same as the sum of two other distances (5.99 Å), indicating the linear structure of  $I_3^-$ . If a bent structure is forced by using 5.85 Å, the peak position of the theoretical scattering curve is not in good agreement with that of the experimental curve. In methanol, the structure of  $I_3^-$  is asymmetric as indicated by a slightly broadened peak at  $\sim 3$  Å, but to a lesser extent than in water, the details of which are shown in the Supplemental Material [30]. Based on this analysis, the symmetry breaking is clearly observed in water and weakly present in methanol, but does not exist in acetonitrile.

In the EXAFS study of the  $I_3^-$  ion in various solvents, it was found that the peak at  $\sim 3$  Å in the scattering curve of the  $I_3^-$  ion exhibits broadening in protic solvents with hydrogen-bonding abilities [22]. In that study, the broadening was attributed to the high Debye-Waller (DW) factor, not to the symmetry breaking caused by solvent-solute interaction. A high DW factor can cause such broadening due to increased structural disorder induced by thermal motion. To account for the possible contribution of a large DW factor to the broadening of the peak at 3.16 Å, we included the DW factor as an additional parameter for the data analysis. When the DW factor was adjusted freely, its relative contribution becomes negligible, suggesting that there is no additional broadening caused by the DW factor. As shown in Fig. 4(c), if we assume that the broadening only arises from the DW factor and there is only one I-I distance, the broad peak at 3.16 Å is still fit well. However, the peak at 6.13 Å also becomes broad and the overall quality of the fit becomes worse, confirming that the broad feature in water does not arise from a high DW factor but from two unequal bond lengths. In this way, the width of  $R_3$  can act as criteria for distinguishing the origin of the broadening.

TABLE I. Structural parameters extracted from the data analysis and DFT calculation.  $R_1$ ,  $R_2$ , and  $R_3$  are the bond distances of  $I_3^-$  ion and  $R_4$  is the bond length of the  $I_2^-$  fragment.

	$R_1$ (Å)	$R_2$ (Å)	$R_1 - R_2$ (Å)	$R_3$ (Å)	$\angle I_1 I_2 I_3$ (deg)	$R_4$ (Å)
Water	$3.38 \pm 0.03$	$2.93 \pm 0.03$	$0.45 \pm 0.04$	$6.13 \pm 0.14$	153	$3.43 \pm 0.03$
Water (DFT calculation)	3.21	2.74	0.47	5.94	172	...
Acetonitrile	$3.01 \pm 0.04$	$2.98 \pm 0.04$	$0.03 \pm 0.06$	5.99 <sup>a</sup>	180	$3.24 \pm 0.06$
Methanol	$3.03 \pm 0.04$	$2.94 \pm 0.03$	$0.09 \pm 0.05$	5.97 <sup>a</sup>	180	$3.59 \pm 0.04$

<sup>a</sup>The maximum value of  $R_3$  was set to be  $R_1 + R_2$  to avoid physically unacceptable structure. The  $R_3$  values for the acetonitrile and methanol solvent hit the limit.



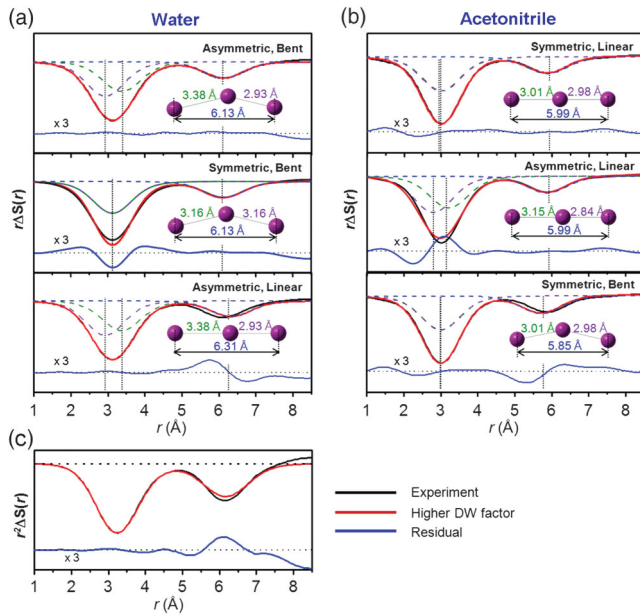


FIG. 4 (color). Structure reconstruction of  $I_3^-$  ion based on the extracted bond distances. The contribution of  $I_3^-$  alone (black solid line) was extracted (see the Supplemental Material [30] for details). Theoretical curves (red) were generated by a sum of three I–I distances (dashed lines). The residuals (blue solid line) are displayed at the bottom. (a) In water solution, the theoretical curve calculated from the asymmetric and bent structure gave the best fit to the experimental curve (top panel). When one average distance (3.16 Å) instead of two unequal distances was used, the broad feature in the experimental curve cannot be matched (middle panel). When a linear and asymmetric structure is used, the sum of two I–I distances (6.31 Å) do not match the  $R_3$  (6.13 Å) determined from the experimental scattering curve, indicating the bent structure (bottom panel). (b) In acetonitrile solution, a symmetric and linear structure gave the best fit (top panel). If two unequal distances (3.15 Å and 2.84 Å) were used, the theoretical curve becomes broader than the experimental curve (middle panel). When a bent structure was used, the peak at 5.99 Å is shifted to a smaller value, giving a worse fit to the experimental curve (bottom). (c) The simulation using a higher DW factor is compared with the experimental curve. For clarity,  $r^2\Delta S(r)$  is used. If a higher DW factor with equal I–I bond lengths was used to fit the broad feature of the peak around 3.16 Å, the peak around 6.13 Å became too broad to fit the experimental curve and the entire quality of the fit became worse (blue).

Our experimental results well account for the results of the previous experimental and theoretical studies. For example, the I–I–I angle of the bent  $I_3^-$  ion in water was estimated to be  $153^\circ$  from transient anisotropy measurement [12]. This estimated value well matches the value extracted from our data. Also, a theoretical study using MD simulation [21] suggested an asymmetric structure of  $I_3^-$  in water with one bond longer by  $0.49$  Å than the other. This prediction is very similar to the result of our measurement ( $0.45$  Å).

In order to find the origin of the symmetry breaking, many theoretical studies have been performed. Although theoretical studies using MD or Monte Carlo simulation have ascribed the origin of the symmetry breaking of  $I_3^-$  in protic solvents to the hydrogen-bonding interaction between solute and solvent molecules, the structure of  $I_3^-$  with broken symmetry has never been optimized by quantum chemical calculation, mainly due to the difficulty of including explicit hydrogen-bonding interaction in the quantum chemical calculation [18–21]. Sato *et al.* found the flattening of the ground-state free-energy surface in aqueous solution [17], but could not find an asymmetric structure as a minimum. In our work, we calculated the molecular structure of  $I_3^-$  by using the density functional theory (DFT) method by considering 34 explicit water molecules (see the Supplemental Material [30] for the computation details). This approach is similar to a recent theoretical investigation of small molecules inside ice nanotube [43]. The optimized structure yielded an asymmetric and bent structure of  $I_3^-$  ion. The structural parameters of the optimized structure are summarized in Table I. The difference between two I–I bond distances ( $0.47$  Å) is well matched with that from the scattering experiment ( $0.45$  Å). We note that the configuration of water molecules displayed in Fig. 5 is not the only possible solution because the solvent molecules fluctuate significantly in reality. Still, it can be seen that the elongated iodine atom has more negative charge than normal and thus can strongly interact with the adjacent hydrogen atoms through hydrogen-bonding interaction. As a result, the solvated ion with broken symmetry can have much lower energy than the symmetric structure in the same solvation environment, as shown in Fig. 5. This DFT calculation confirms that the symmetry breaking of the  $I_3^-$  ion is induced by hydrogen-bonding interaction.

In summary, by applying time-resolved x-ray solution scattering, we characterized the structure of the  $I_3^-$  ion in three different solvents, elucidating subtle structural changes of the ion depending on the hydrogen-bonding ability of the solvent. In water solution, we found that the

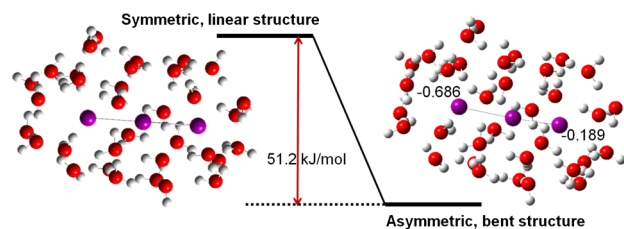


FIG. 5 (color online). Optimized structures and the relative energies of  $I_3^-$  ion with 34 explicit water molecules forming the first solvation shell by DFT method (see the Supplemental Material [30]). The optimized structure of  $I_3^-$  ion has a broken symmetry (asymmetric, bent) and is stabilized by  $51.2$  kJ/mol compared with the linear symmetric one. The elongated iodine atom has a higher negative charge.

$I_3^-$  ion takes an asymmetric and bent structure, lowering the structural symmetry. This phenomenon is also weakly present in methanol but not in acetonitrile. Our results provide direct evidence for broken symmetry of the triiodide ion in hydrogen-bonding solvents and clarify the subtle effect of solute-solvent interaction on the structure of ionic species.

We thank Shin-ya Koshihara for his support. This work was supported by the Research Center Program (CA1201) of IBS (Institute for Basic Science) in Korea, by PRESTO/JST, and by an Inha University Research Grant (INHA-46438). This work was carried out with the approval of the Photon Factory Program Advisory Committee (Proposal No. 2009S2-001 and No. 2010G553).

\*Corresponding author.

shinichi.adachi@kek.jp

†Corresponding author.

hyotcherl.ihee@kaist.ac.kr

- [1] S. Koneshan, J. C. Rasaiah, R. M. Lynden-Bell, and S. H. Lee, *J. Phys. Chem. B* **102**, 4193 (1998).
- [2] K. Modig, E. Liepinsh, G. Otting, and B. Halle, *J. Am. Chem. Soc.* **126**, 102 (2004).
- [3] E. Gouaux and R. MacKinnon, *Science* **310**, 1461 (2005).
- [4] D. E. Moilanen, D. Wong, D. E. Rosenfeld, E. E. Fenn, and M. D. Fayer, *Proc. Natl. Acad. Sci. U.S.A.* **106**, 375 (2009).
- [5] I. A. Heisler and S. R. Meech, *Science* **327**, 857 (2010).
- [6] D. Laage, G. Stirnemann, F. Sterpone, R. Rey, and J. T. Hynes, *Annu. Rev. Phys. Chem.* **62**, 395 (2011).
- [7] U. Banin, A. Waldman, and S. Ruhman, *J. Chem. Phys.* **96**, 2416 (1992).
- [8] U. Banin and S. Ruhman, *J. Chem. Phys.* **98**, 4391 (1993).
- [9] T. Kuhne, R. Kuster, and P. Vohringer, *Chem. Phys.* **233**, 161 (1998).
- [10] L. Zhu, K. Takahashi, M. Saeki, T. Tsukuda, and T. Nagata, *Chem. Phys. Lett.* **350**, 233 (2001).
- [11] A. E. Johnson and A. B. Myers, *J. Phys. Chem.* **100**, 7778 (1996).
- [12] T. Kuhne and P. Vohringer, *J. Phys. Chem. A* **102**, 4177 (1998).
- [13] P. W. Anderson, *Science* **177**, 393 (1972).
- [14] G. Z. Liu and G. Cheng, *Phys. Rev. B* **65**, 132513 (2002).
- [15] L. D. Landau and E. M. Lifshitz, *Statistical Physics* (Pergamon, Oxford, 1969).
- [16] Y. Ogawa, O. Takahashi, and O. Kikuchi, *J. Mol. Struct.* **424**, 285 (1998).
- [17] H. Sato, F. Hirata, and A. B. Myers, *J. Phys. Chem. A* **102**, 2065 (1998).
- [18] C. J. Margulis, D. F. Coker, and R. M. Lynden-Bell, *Chem. Phys. Lett.* **341**, 557 (2001).
- [19] C. J. Margulis, D. F. Coker, and R. M. Lynden-Bell, *J. Chem. Phys.* **114**, 367 (2001).
- [20] T. Koslowski and P. Vohringer, *Chem. Phys. Lett.* **342**, 141 (2001).
- [21] F. S. Zhang and R. M. Lynden-Bell, *Phys. Rev. Lett.* **90**, 185505 (2003).
- [22] H. Sakane, T. Mitsui, H. Tanida, and I. Watanabe, *J. Synchrotron Radiat.* **8**, 674 (2001).
- [23] E. Collet *et al.*, *Science* **300**, 612 (2003).
- [24] A. Makal, E. Trzop, J. Sokolow, J. Kalinowski, J. Benedict, and P. Coppens, *Acta Crystallogr. Sect. A* **67**, 319 (2011).
- [25] S. Tornroth-Horsefield, Y. Wang, K. Hedfalk, U. Johanson, M. Karlsson, E. Tajkhorshid, R. Neutze, and P. Kjellbom, *Nature (London)* **439**, 688 (2006).
- [26] K. Istomin, V. Kotaidis, A. Plech, and Q. Y. Kong, *Appl. Phys. Lett.* **90**, 022905 (2006).
- [27] P. Lindqvist-Reis, K. Lamble, S. Pattanaik, I. Persson, and M. Sandstrom, *J. Phys. Chem. B* **104**, 402 (2000).
- [28] M. Matsugami, T. Takamuku, T. Otomo, and T. Yamaguchi, *J. Phys. Chem. B* **110**, 12372 (2006).
- [29] T. Takamuku, H. Maruyama, S. Kittaka, S. Takahara, and T. Yamaguchi, *J. Phys. Chem. B* **109**, 892 (2005).
- [30] See Supplemental Material at <http://link.aps.org/supplemental/10.1103/PhysRevLett.110.165505> for methods and figures.
- [31] J. Davidsson *et al.*, *Phys. Rev. Lett.* **94**, 245503 (2005).
- [32] H. Ihee, M. Lorenc, T. K. Kim, Q. Y. Kong, M. Cammarata, J. H. Lee, S. Bratos, and M. Wulff, *Science* **309**, 1223 (2005).
- [33] A. Plech, V. Kotaidis, M. Lorenc, and J. Boneberg, *Nat. Phys.* **2**, 44 (2006).
- [34] M. Christensen, K. Haldrup, K. Bechgaard, R. Feidenhans'l, Q. Kong, M. Cammarata, M. Lo Russo, M. Wulff, N. Harrit, and M. M. Nielsen, *J. Am. Chem. Soc.* **131**, 502 (2009).
- [35] S. Westenhoff *et al.*, *Nat. Methods* **7**, 775 (2010).
- [36] M. Christensen, K. Haldrup, K. Bechgaard, R. Feidenhans'l, Q. Kong, M. Cammarata, M. Lo Russo, M. Wulff, N. Harrit, and M. M. Nielsen, *J. Am. Chem. Soc.* **131**, 502 (2009).
- [37] K. Haldrup, M. Christensen, M. Cammarata, Q. Kong, M. Wulff, S. O. Mariager, K. Bechgaard, R. Feidenhans'l, N. Harrit, and M. M. Nielsen, *Angew. Chem., Int. Ed.* **48**, 4180 (2009).
- [38] S. Jun, J. H. Lee, J. Kim, K. H. Kim, Q. Kong, T. K. Kim, M. Lo Russo, M. Wulff, and H. Ihee, *Phys. Chem. Chem. Phys.* **12**, 11536 (2010).
- [39] H. Ihee, *Acc. Chem. Res.* **42**, 356 (2009).
- [40] T. K. Kim, J. H. Lee, M. Wulff, Q. Y. Kong, and H. Ihee, *ChemPhysChem* **10**, 1958 (2009).
- [41] Q. Kong, J. H. Lee, K. H. Kim, J. Kim, M. Wulff, H. Ihee, and M. H. Koch, *J. Am. Chem. Soc.* **132**, 2600 (2010).
- [42] S. Nozawa *et al.*, *J. Synchrotron Radiat.* **14**, 313 (2007).
- [43] R. M. Kumar, M. Elango, R. Parthasarathi, and V. Subramanian, *J. Phys. Chem. A* **115**, 12841 (2011).